TERRA LATINOAMERICANA

Why Does Clay Soil Have Low Cation Exchange Capacity? Mineral and Elemental Composition of Silts and Clays
¿Por Qué un Suelo Arcilloso Tiene Baja Capacidad de Intercambio Catiónico? Composición Mineral y Elemental de Limos y Arcillas

Antonio López-Castañeda[1], Álvaro de Jesús Ruíz-Baltazar[2], David Jesús Palma-López[1], Joel Zavala-Cruz[1] y Francisco Bautista-Zuñiga[3‡]

[1] Colegio de Postgraduados, Campus Cárdenas, Tabasco. Periférico Carlos A. Molina s/n. 86500, H. Cárdenas, Tabasco, México; (A.L.C.), (D.J.P.L.), (J.Z.C.).
[2] SECIHTI-Universidad Nacional Autónoma de México, Centro de Física Aplicada y Tecnología Avanzada. Boulevard Juriquilla No. 3001. Col. Juriquilla. 76230 Santiago de Querétaro, Querétaro, México; (A.J.R.B.).
[3] Universidad Nacional Autónoma de México, Centro de Investigaciones en Geografía Ambiental. Antigua Carretera a Pátzcuaro No. 8701, Col. Ex Hacienda de San José de la Huerta. 58190 Morelia, Michoacán, México; (F.B.Z).
‡ Corresponding author: leptosol@ciga.unam.mx

SUMMARY

Acidic soils in the Mexican tropics, such as those found in Tabasco, are characterized by fine texture and high organic matter content. However, they exhibit low cation exchange capacity (CEC), which limits their agricultural productivity. This study aimed to identify and characterize, for the first time, the mineralogical and elemental composition of the sand, silt, and clay fractions in an ancient acidic fluvioalluvial soil using X-ray diffraction (XRD), Fourier-transform infrared spectroscopy (FT-IR), energy-dispersive X-ray spectroscopy (EDS), and scanning and transmission electron microscopy (SEM-STEM). Results revealed that the clay fraction is predominantly composed of kaolinite, with secondary phases of gibbsite, magnetite, and iron and aluminum sesquioxides. These oxides absorb onto kaolinite surfaces, further reducing its CEC. The silt fraction was primarily composed of Al, Si, Fe, and C, with very low concentrations of Ca and Mg, indicating a limited natural nutrient reserve. Notably, small amounts of organic matter were detected in both sand and silt fractions, forming organo-mineral complexes potentially stabilized by interactions with metallic oxides, low pH, and seasonal anoxia associated with high annual rainfall (2600 mm). These findings suggest that the low CEC results not only from the mineralogical composition but also from pedoclimatic conditions that limit the soil's chemical reactivity. Although these soils are classified as agricultural classes III and IV, their use is restricted mainly to citrus, cassava, pineapple, and forest plantations. This study provides original evidence on the structure–function relationships of fine fractions in acidic tropical soils. It highlights the importance of considering both mineralogy and geochemistry, not just texture, when designing sustainable soil management strategies in environmentally vulnerable regions.

Index words: *low-activity minerals, metal oxides, organo-mineral complexes, soil fertility, weathering*.

RESUMEN

Los suelos ácidos del trópico mexicano, como los de Tabasco, se caracterizan por su textura fina, alto contenido de materia orgánica y, paradójicamente, baja capacidad de intercambio catiónico (CIC), lo que limita su fertilidad agrícola. Este estudio tuvo como objetivo identificar y caracterizar, por primera vez, la composición mineralógica y elemental de las fracciones de arena, limo y arcilla en un suelo fluvioaluvial antiguo ácido mediante técnicas de difracción de rayos X (DRX), espectroscopía infrarroja por transformada de Fourier (FT-IR), espectroscopía de energía dispersiva

check for updates

Recommended citation:

López-Castañeda, A., Ruíz-Baltazar, Á. J., Palma-López, D. J., Zavala-Cruz, J., & Bautista-Zuñiga, F. (2026). Why Does Clay Soil Have Low Cation Exchange Capacity? Mineral and Elemental Composition of Silts and Clays. *Terra Latinoamericana, 44*, 1-14. e2362. https://doi.org/10.28940/terralatinoamericana.v44i.2362

Received: July 14, 2025.
Accepted: September 25, 2025.
Article, Volume 44.
February, 2026.

Section Editor:
Dra. Dámaris Leopoldina Ojeda-Barrios

Technical Editor:
M.C. Ayenia Carolina Rosales Nieblas

(EDS) y microscopía electrónica de barrido (SEM-STEM). Los resultados revelaron que la fracción arcillosa está compuesta principalmente por caolinita, con presencia secundaria de gibbsita, magnetita y sesquióxidos de hierro y aluminio, los cuales se adsorben a la superficie de la caolinita, reduciendo su CIC. La fracción limo presentó elementos como Al, Si, Fe y C, con bajos niveles de Ca y Mg, lo que indica una reserva nutrimental limitada. De forma novedosa, se detectó materia orgánica en fracciones de arena y limo formando complejos organominerales, posiblemente estabilizados por interacciones con óxidos metálicos, pH bajo y condiciones de anoxia estacional, derivadas de la alta precipitación anual (2600 mm). Estos hallazgos sugieren que tanto la mineralogía dominante como las condiciones edafoclimáticas son responsables de la baja reactividad química del suelo. A pesar de estar clasificados como suelos agrícolas de clase III y IV, su uso está restringido a cultivos como cítricos, yuca, piña y plantaciones forestales. Esta investigación aporta evidencia original sobre la composición y funcionalidad de las fracciones finas en suelos ácidos tropicales y subraya la importancia de considerar no solo la textura, sino también la mineralogía y la geoquímica en el diseño de estrategias de manejo sostenible en regiones ambientalmente vulnerables.

Palabras clave: *minerales de baja actividad, óxidos metálicos, complejos organominerales, fertilidad edáfica, intemperismo.*

INTRODUCTION

Acid soils occupy approximately 30% of the world's ice-free land surface and are found mainly in the northern belt (cold and temperate climate) and the southern tropical belt (von Uexküll and Mutert, 1995). One-third of the tropics (1.7 billion ha) have acid soils with soluble Al to be toxic for most crops (Sánchez and Logan, 1992; Agegnehu *et al*., 2021). Acidic soils belonging to the Acrisols, Alisols, Umbrisols, and Luvisols groups occupy around 6183 km² of surface area in the southern Mexican state of Tabasco. The acid soils in Mexico are used for sowing pastures for extensive cattle ranching, as well as for forest plantations of eucalyptus, tropical pine, rubber, acacia, and teak, and to a lesser extent for oil palm, lemon, orange, and pineapple plantations (Zavala-Cruz, Jiménez, Palma, Bautista, and Gavi, 2016; Palma-López *et al*., 2017).

In the tropics, the low productivity of acidic soils, among other causes, has led to the opening of agricultural lands, which has led to the reduction of forest cover from 49.1% in 1940 to only 13.6% today, with the consequent loss of biodiversity (Villanueva-Partida *et al*., 2016) and has worsened soil erosion and degraded fertility. This environmental degradation underscores the need for sustainable land-use strategies that consider the unique physicochemical properties of the region's soils. In recent decades, rapid urbanization, agricultural expansion, and industrial activities, including oil extraction, have dramatically altered the environment in southern Mexico. These activities have led to heavy metal contamination in various ecosystems, including soils, rivers, and coastal lagoons (Marín-Mézquita, Baeza, Zapata, and Gold, 1997; Villasenor et al., 2003; Geissen *et al*., 2009; Mendoza-Carranza, Sepúlveda, Dias, and Geissen, 2016).

In Tabasco, Mexico, where agricultural practices heavily depend on soil quality, contaminants originating partly from agrochemicals and industrial waste represent significant risks for crop production and food security (Geissen *et al.,* 2009). Understanding how these soils interact with contaminants and how their mineral composition influences these interactions is key to developing strategies that mitigate soil degradation and ensure sustainable agricultural practices. In addition, unsustainable agricultural management practices have led to soil degradation through erosion or fertility loss.

Acidic soils in Tabasco, Mexico, as in other parts of the world, have low productivity, despite being clayey and having high percentages of organic matter; the cation exchange capacity is very low (Zavala-Cruz *et al.,* 2016). The agricultural interpretation of soil texture has not been correct due to the lack of knowledge of the type of minerals in particles smaller than 2 microns.

Although there are isolated reports on the sedimentary composition of sands in Tabasco and broader studies on coastal sediments in nearby regions (Ramos-Vázquez and Armstrong, 2020), there is a notable lack of comprehensive analyses of moisture retention and CEC in these soil components. Additionally, the mineralogical composition of these soils, including the identification of clay minerals like kaolinite, smectite, and illite, remains largely unexplored.

For example, Castillo, Popma, and Moreno-Casasola (1991) noted differences in vegetation between siliceous and carbonate dunes in Tabasco and Campeche. However, these studies did not address the soil's mineral composition or water retention behavior. Without such information, interpretations of soil texture and fertility for agricultural purposes remain incomplete and potentially misleading. Despite their importance, most previous research has focused on the general texture of these soils, overlooking critical factors such as moisture retention, cation exchange capacity (CEC), and mineral interactions. These factors are essential for understanding soil fertility and improving agricultural management.

Sustainable soil management in agriculture needs a thorough knowledge of silt and clay types and their elemental composition. We have an intuition, but scientific evidence is scarce. Special attention is given to their mineral composition, water retention capacity, and cation exchange potential. These findings will contribute to developing soil management strategies to enhance agricultural sustainability, improve crop yields, and mitigate the environmental impacts of land-use change in one of Mexico's most productive and environmentally vulnerable regions.

Understanding the composition and behavior of sand particles (Miaomiao, Yulong, Xirui, Xuhui, and Mengzhen, 2021), silts particles (Liu *et al*., 2020; Nie, Li, Wang, and Bai, 2020), and clays particles (Adhikari and Bhattacharyya, 2015; Zhu *et al*., 2021) in these soils are essential for designing management practices that mitigate the adverse effects of deforestation and improve agricultural productivity. Sustainable practices depend on detailed soil characterizations, including moisture retention, mineral content, and cation exchange capacity, which are vital for determining irrigation, fertilization, and crop selection (Djeran-Maigre, Tessier, Gravaud, Gouy, and Belarbi, 2023)

We need to pay special attention to their mineral and elemental composition. These findings will contribute to developing soil management strategies to enhance agricultural sustainability, improve crop yields, and mitigate the environmental impacts of land-use change in one of Mexico's most productive and environmentally vulnerable regions.

This work aimed to identify and characterize sand, silts and clays particles of an acid soil profile in Tabasco, Mexico, through mineralogical and elemental analysis.

MATERIALS AND METHODS

Study Area

The state of Tabasco is in southeastern Mexico. It covers 24 751 km^2 between the coordinates 17° 15′ and 18° 38′ N and 90° 38′ and 94° 07′ W (Figure 1). The state comprises two physiographic provinces: the Southern Gulf Coastal Plain, which covers 96% of the area, and the Sierras of Chiapas and Guatemala, which cover the remaining 4%. Both provinces are drained by the basins of the Usumacinta and Grijalva rivers, which together contribute 30% of the country´s 's freshwater to the Gulf of Mexico. The soil profile under study is in the Southern Gulf Coastal Plain physiographic province (17° 52' 21.92" N - 93° 40' 0.41" W), with a gently rolling hilly landscape (Zavala-Cruz *et al*., 2016). It has a warm, humid climate with year-round rainfall (Af (m), a mean annual temperature of 25.5 °C, and an average annual precipitation of 2600 mm (Aceves-Navarro and Rivera, 2019). The parental material is sand and silt from the Quaternary Pleistocene (Islas-Tenorio *et al*., 2005).

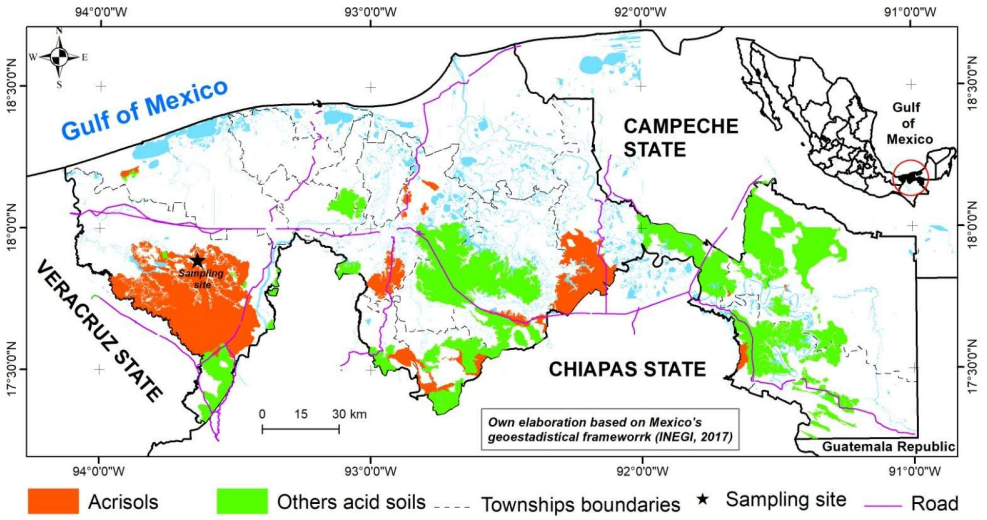

Figure 1. Study area: the acidic soils of Tabasco.

Particle Separation Techniques

For particle analysis, an Acrisol profile with a high organic matter content, clayey, and acidic, was selected (Salgado-García *et al*., 2017) (Table 1). Soil samples from each horizon were dried in the shade for 48 hours. The soil samples were sieved through a 10-mesh sieve (2 mm gap). The sand was separated by dry sieving through a 250-mesh sieve (0.063 mm). The silt was separated wet using a sodium hexametaphosphate solution as a dispersant and mechanical stirring for 5 min. The soil sample was allowed to stand for 2 for the silt to decant; clays were obtained from the supernatant. Clay and silt particles were separately placed on filter paper and dried in the shade for 5 days.

The sand, silt, and clay samples were analyzed using a High-Resolution Scanning Electron Microscopy (HR-SEM) model Hitachi SU8030. Employing secondary electron (SE) imaging to obtain detailed micrographs of the nanostructures within the soil particles using a High-Resolution Scanning Electron Microscopy (HR-SEM).

Mineralogical Analysis (XRD)

Structural analysis was carried out using X-ray diffraction (XRD) with a Rigaku Ultima IV X-ray Diffractometer. The samples were scanned in the 10° to 90° 2θ range with a Cu Kα radiation wavelength of 1.54 Å and a scanning speed of 0.02°/min. X-ray diffraction (XRD) patterns of clay particles from the first three soil horizons (H1, H2, and H3) were analyzed. To determine the relative abundance of each mineral phase, a phase quantification analysis (QPA) was conducted. This technique provided essential data on the soil nanostructures´ crystallographic structure, phase composition, and crystallite size.

Morphochemical Analysis (SEM, EDS, FT-IR).

Energy dispersive X-ray spectroscopy (EDS) was utilized with an operating voltage of 15 kV and a working distance of 15 mm. It was used for elemental composition mapping and detailed chemical characterization of the three particle size fractions (sand, silt and clay) of the acid soil. The Bruker X Flash 6/60 EDS system was coupled with the Hitachi SU8230 field emission scanning electron microscope.

Transmission-mode scanning electron microscopy (STEM) was conducted using the Hitachi SU8230 cold-field emission scanning electron microscope to detail the morphologies of the silt and clay particles. In order to abound in depth, regarding the size and morphology of the clay, a complementary scanning transmission electron microscopy (STEM) analysis was performed.

FT-IR analysis was conducted using a Nicolet iN10 spectrometer with an ATR accessory, recording spectra from 400 to 4000 cm^{-1}. The ATR mode enabled direct solid sample analysis, enhancing signal quality and reproducibility. This allowed precise identification of vibrational modes associated with the mineral phases in the soil sample, complementing XRD results.

Table 1. Physical and chemical properties of the acid soil profile.

Horizon Depth	R	L	A	pH	OM	N	P	K	Ca	Mg	Na	CIC	CEC-R	H	Al
		%		H_2O	%		mg kg^{-1}	- - - - - - - - - - - - - - - cmol(+) kg^{-1} - - - - - - - - - - - - - - -							
0-15	37	11	52	4.52	5.61	0.19	8.10	0.71	0.58	0.38	0.08	7.15	19.32	1.47	3.11
15-(30-40)	40	8	52	4.42	2.51	0.07	1.47	0.15	0.08	0.07	0.04	4.10	10.25	1.09	2.82
(30-40) -57	41	6	53	4.43	1.90	0.05	0.59	0.07	0.06	0.03	0.03	4.76	11.61	0.99	2.37
57-114	46	7	47	4.41	0.43	0.02	0.00	0.04	0.46	0.23	0.05	5.53	12.02	0.76	1.88
114-150	45	10	45	4.19	0.10	0.01	0.29	0.02	0.13	0.17	0.04	7.15	15.89	0.99	2.57

OM = organic matter; N = total; CEC = cation exchange capacity; R = clay, L = silt; A = sand.

RESULTS AND DISCUSSION

Form, Sizes, and Composition of Sand Particles (250 to 2000 microns)

Using secondary electrons, the micrograph obtained with scanning electron microscopy (SEM) reveals the morphology of sand grains, with sizes of 280 µm and 365 µm (Figure 2a). Depicts of an elemental mapping of the same sand grains highlight key elements, including silicon (Si) and oxygen (O). Also, aluminum (Al) and iron (Fe) are in low proportions (Figure 2b). These elements are primarily associated with quartz minerals and indicate the presence of iron and aluminum oxides (Al-oxides). Sands with quartz and iron minerals were probably produced by the weathering of ash from the Chichonal volcano in Chiapas.

The Energy Dispersive X-ray Spectroscopy (EDS) spectrum confirms the presence of Si, O, Al, and Fe alongside a minor peak for carbon (C) (Figure 2c). The detected carbon may be attributed to trace organic components within the sand fraction, representing a minor phase relative to the predominant inorganic minerals.

Figures 2 (d-h) illustrates the individual elemental distributions for Si, O, Fe, Al, and C. These distributions reinforce the associations of Si and O with quartz as principal components. In contrast, the distributions of Fe and Al correspond to the presence of iron and aluminum oxides in low proportions. The minor presence of carbon suggests localized organic matter or carbon-bearing phases, aligning with the observations from the EDS spectrum. Carbon in the sand grains indicates that these particles are reactive and can form organo-mineral compounds.

To our surprise, we found that the sand fraction presented small quantities of organic matter forming organo-mineral compounds, as well as in silt fraction; the sand and silt are reactive as has also been reported for tropical soils (Soares, Alleoni, Vidal-Torrado, and Cooper, 2005; Thaymuang, Kheoruenromne, Suddhipraharn, and Sparks, 2013), perhaps because of the minerals coming from the weathering of the ash from the Chichonal volcano, the presence of organic matter bound to the sands is probably related to the interaction with iron and aluminum oxides, as well as with the inhibition of mineralization due to low pH and Al-toxicity and by the persistent anaerobiosis in the copious rainy season in the area (Mora, Guerra, Armas, Arbelo, and Rodríguez, 2014) and by the formation of organo-minerals complex (Hassink, 1997; Prado *et al*., 2007; Delmelle, Opfergelt, Cornelis y Ping, 2015). However, this hypothesis will need to be tested in future studies.

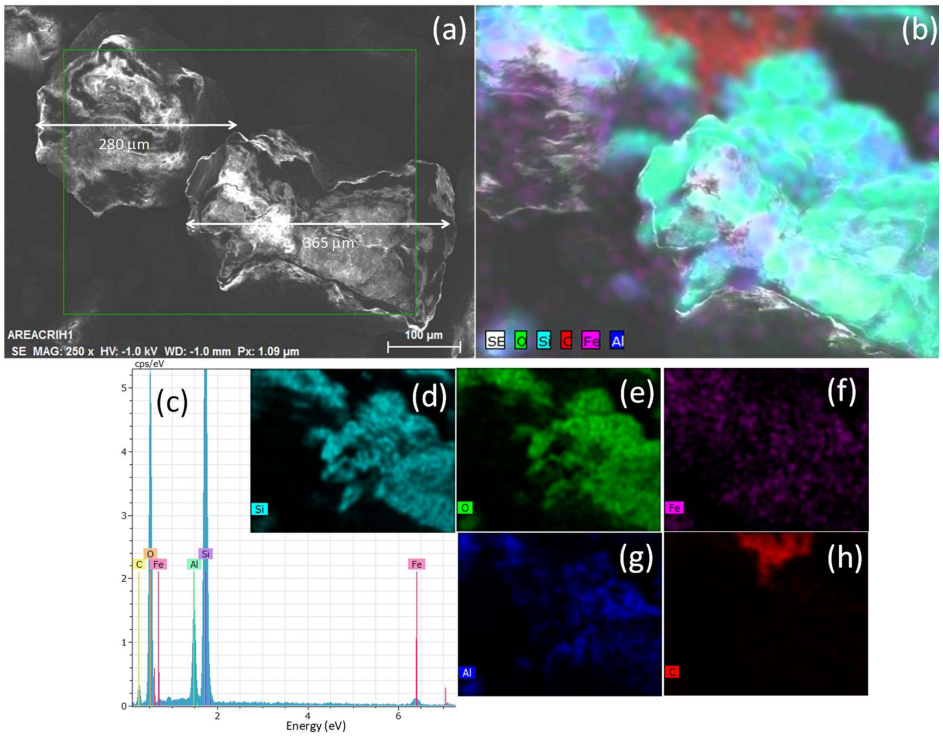

Figure 2. Characterization of sands of acid soil from Tabasco, Mexico. (a) SEM image showing sand grains sized approximately 280 µm and 365 µm. (b) Elemental mapping indicates the presence of silicon (Si), oxygen (O), aluminum (Al), and iron (Fe). (c) EDS spectrum confirming Si, O, Al, Fe, and a minor carbon (C), (d-h) Individual elemental distributions for Si, O, Fe, Al, and C.

Form, Sizes and Composition of Silt Particles (2 to 63 microns)

The EDS spectrum reveals the presence of elements such as O> Al> Si> C>Fe> Ag> Na> Ti> Mg> Ca. These elements are associated with the primary and secondary minerals present in the silt and clay particles (Figure 3a). Important elements for plant nutrition, such as calcium and magnesium, are found in low proportions.

The presence of silver may be associated with specific interactions with minerals or organic matter, while iron may be associated with iron oxide phases, characteristic of acidic soils. The distribution of carbon suggests the formation of organometallic complexes on the surface of the mineral phases (Figure 3b). Note that the silt-sized particle is associated with primary and secondary minerals, such as iron oxides, and organic compounds. The large particle is an organo-mineral compound (Feng, Zhang, Wang, and Li, 2023) containing carbon, silver, and iron as the main elements (Figure 3b). A strong interaction was observed between the organo-mineral component (silver-carbon) and the smallest particles of iron oxides.

Figure 3c shows a secondary electron image obtained with the EDS spectrum. Figures 3(d-f) show the individual EDS spectra of silver (Ag), iron (Fe), and carbon (C), respectively. These maps confirm the distribution of these elements on the mineral surfaces, suggesting a relationship between the presence of the silt-sized particle and the clay-sized particle assemblage.

As expected in acidic tropical soils, the silt fraction is composed primarily of Al, Si, C, and Fe, with low concentrations of nutrients such as Ca and Mg. Natural, long-term fertility is found in the chemical composition of silt, which, in this case, contributes minor amounts of Ca^{2+} and Mg^{2+}. These results on the composition of silts are the first for these acidic soils of the Mexican tropics.

Research on the nutrient content of sand and silt has unfortunately not been so popular; scientific reports on the subject are scarce despite the great relevance they have for achieving sustainable agriculture, since the release of nutrients in the medium and long term should be relevant (Graham, 1943; Bremner and Genrich, 1990; Hassink, 1997; Delmelle *et al*., 2015).

Form, Sizes and Composition of Clay Particles (<2 microns)

SEM images, a significant tool in our research, not only reveal but also confirm the presence and morphology of kaolinite, as well as iron and aluminum oxides, on soil particles smaller than 2 microns (Figure 4a-d). Figure 4a shows a secondary electron (SE) SEM image acquired at 25 000× magnification and 1 kV accelerating voltage. In this image, pseudohexagonal kaolinite platelets forming loose aggregates are observed. In addition, dispersed clusters of irregularly shaped particles are observed, which could be associated with iron and aluminum oxides. The presence of these oxides is a well-documented feature of acidic soils, where weathering processes promote the accumulation of sesquioxides, influencing the structure and chemical properties of the soil.

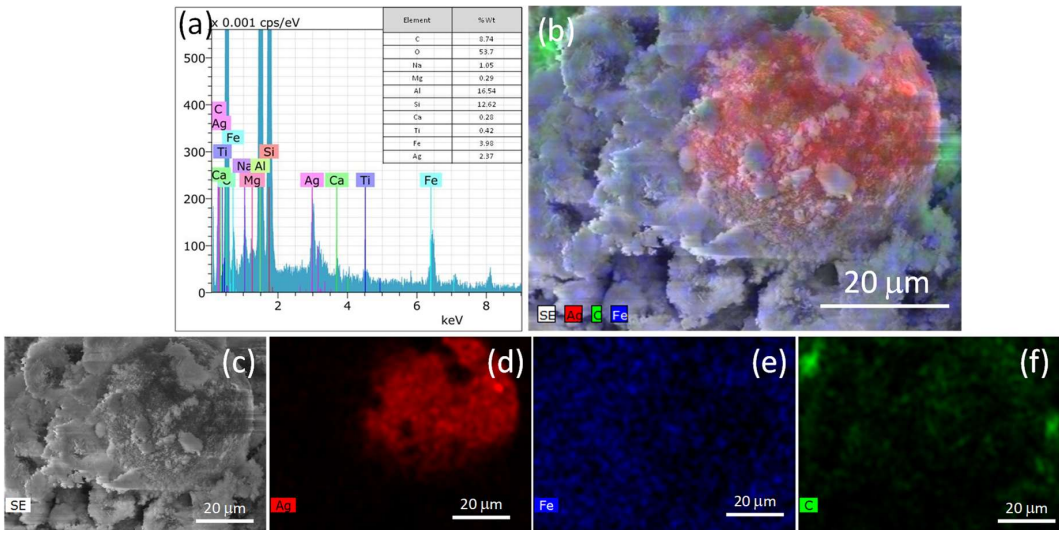

Figure 3. Elemental analysis of silt-clay particles using EDS. (a) EDS spectrum showing the presence of Si, O, Al, Mg, Ca, Fe, and Ag. (b) Focused EDS spectrum highlighting silver (Ag), iron (Fe), and carbon (C). (c) Secondary electron (SE) image of the sample region analyzed. (d) EDS spectrum for silver (Ag), (e) iron (Fe), and (f) carbon (C).

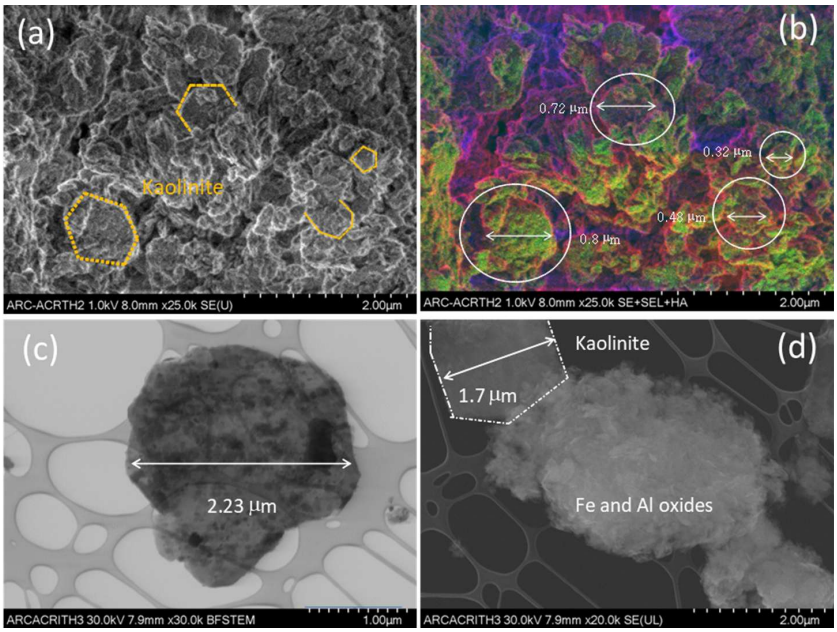

Figure 4. (a) SE-SEM image (25,000×, 1 kV) showing pseudohexagonal kaolinite platelets and iron-aluminum oxide clusters. (b) Multimodal imaging (SE, BSE, HAADF) enhancing phase contrast. (c) BF-STEM image (30 000×) revealing kaolinite morphology and submicron oxide inclusions. (d) SE-UL image confirms kaolinite and iron-aluminum oxide coexistence in acidic soils.

Our research methodology is meticulous, as we obtained a more detailed view of the kaolinite morphology through a combination of SE, backscattered electron (BSE), and high-angle annular dark field (HAADF) imaging modes at the same magnification (25 000×) (Figure 4b). This multimodal approach enhances contrast, allowing for more precise differentiation between kaolinite and the other coexisting mineral particles. Particle size measurements indicate that kaolinite platelets exhibit dimensions below 1 µm, a defining characteristic of clay minerals. This observation is consistent with the mineralogical composition expected for the acidic soils of Tabasco, where kaolinite is the predominant aluminosilicate.

Brightfield scanning transmission electron microscopy (BF-STEM) imaging at 30 000× magnification provides a higher-resolution view of the pseudohexagonal morphology of kaolinite (Figure 4c). Submicron inclusions can be discerned within these structures, corresponding to iron and aluminum oxides embedded in the clay matrix. These oxide inclusions suggest that kaolinite may act to adsorb secondary mineral phases, potentially contributing to decreased cation exchange capacity. Clay-sized particles are also observed, a collection of iron and aluminum oxides and hydroxides that form silt-sized particles larger than 2 microns.

The SE-UL (secondary low-angle electron) image provides improved visual resolution of the coexisting morphological features. Both pseudohexagonal kaolinite structures and agglomerates associated with iron and aluminum oxides can be distinguished (Figure 4d). The coexistence of these two morphologies further corroborates the heterogeneous mineralogical composition of the acidic soil particles in Tabasco, where kaolinite-rich domains coexist with iron- and aluminum-containing phases. This biphasic nature, particularly the presence of kaolinite, contributes to the unique physicochemical properties of these soils, influencing their low fertility, hydrological behavior, and low heavy metal adsorption.

These findings reinforce the understanding of acidic soils as highly weathered systems dominated by kaolinite and iron and aluminum oxides (sesquioxides), which collectively dictate their agricultural potential and environmental interactions.

We used EDS in STEM mode of scanning electron microscopy to clarify the presence of aluminum and iron oxide in the clay particles. The figure shows an EDS spectrum revealing the primary presence of elements such as Si, O, Al, and Fe (Figure 5a). This result supports the findings previously observed in the micrographs and confirms that kaolinite is the main aluminosilicate. The scanning electron microscopy (SEM) image of the clay-sized particle sample at 70 000x magnification reveals the presence of kaolinite with a suite of much smaller iron and aluminum oxides adsorbed on the surface (Figure 5b). Finally, Figure 5c shows the elemental mapping of the crucible, further verifying the particle composition.

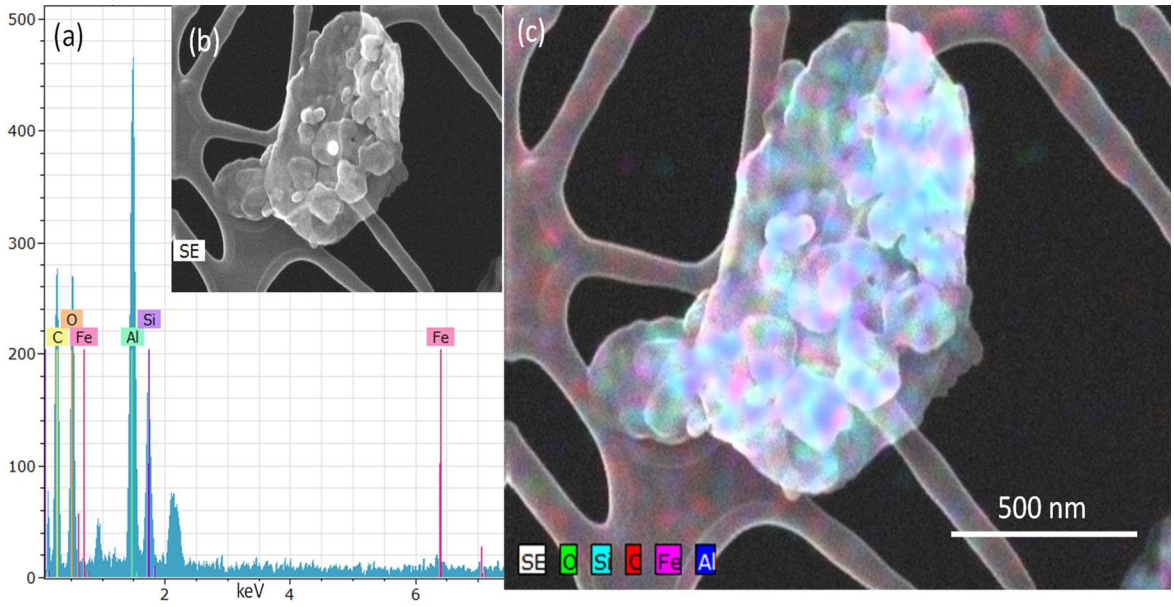

Figure 5 (a-c): EDS analysis in STEM mode. (a) EDS spectrum showing the primary elements Si, O, Al, and Fe. (b) SEM image of soil particles at 70,000x magnification. (c) Elemental mapping verifying kaolinite as the main component of acidic soils from Tabasco.

To improve our understanding of the clay particle microstructure, we used various scanning electron microscopy (SEM) techniques, each of which shows distinctive contrast variations. For example, Figure 6a shows a Bright Field Transmission Electron Microscopy (BSM) image, which reveals transparent kaolinite phases, indicating their lower electron density; such transparency suggests that the kaolinite particles are approximately 500 nm in size. Figure 6b highlights the surface topography and provides morphological information of the clay particles.

In the High-Angle (HA(T)) image, emphasizing denser components such as iron and aluminum oxides, which appear darker due to their higher atomic numbers (Figure 6c). Finally, presents a composite image representing the superposition of SE, BFTEM, and HA(T) modes, offering a comprehensive view of the sample (Figure 6d).

Figures 4, 5, and 6 show that the kaolinite particles, the largest, have small particles of iron and aluminum oxides on their surface, which makes us think that we have probably been measuring the cation exchange capacity incorrectly by obtaining values lower than 7 cmol(+) kg^{-1} soil or clay? due to the occlusion of the aluminosilicates by the iron and aluminum oxides.

Crystalline Clay Minerals Identify in Depth

Diffraction peaks were indexed and fully identified based on reference diffraction cards for kaolinite (00-014-0164), gibbsite (04-013-6979), montmorillonite (00-060-0318), and magnetite (01-091-6177) (Figure 7a). The diffraction patterns reveal that kaolinite is the predominant crystalline phase in the clay particles of all three horizons, with well-defined reflections corresponding to its characteristic basal planes. Gibbsite and magnetite were also identified in variable proportions, while montmorillonite was only detected in H1. Specifically, the main peaks and planes diffraction identified for each mineralogical phase were as follows: kaolinite; 12.41° (001), 19.87 (020), 20.38° (110), 21.23 (111) and 24.97° (002); gibbsite; 18.3° (020), 20.32° (110), 36.51° (311); magnetite; 18.20° (111), 30.09° (202), 35.44° (311), 43.08° (400).

Kaolinite was the major component of clay crystalline particles in all three horizons, with concentrations ranging from 80.9% to 85.8% (Figure 7b). Gibbsite content ranged from 6.2% to 9.4%, while magnetite showed greater variability, with values ranging from 0.3% in H1 to 10.2% in H2. Montmorillonite was present exclusively in H1 (7.7%).

These results are consistent with the morphological and structural observations obtained from scanning electron microscopy (SEM), where the characteristic platy morphology of kaolinite was identified. The presence of well-defined kaolinite diffraction peaks further corroborates the SEM findings, supporting the identification of this mineral as a significant constituent in the studied soils. The predominance of kaolinites suggests a highly weathered soil environment, typical of acidic tropical soil with significant leaching and aluminum-iron enrichment.

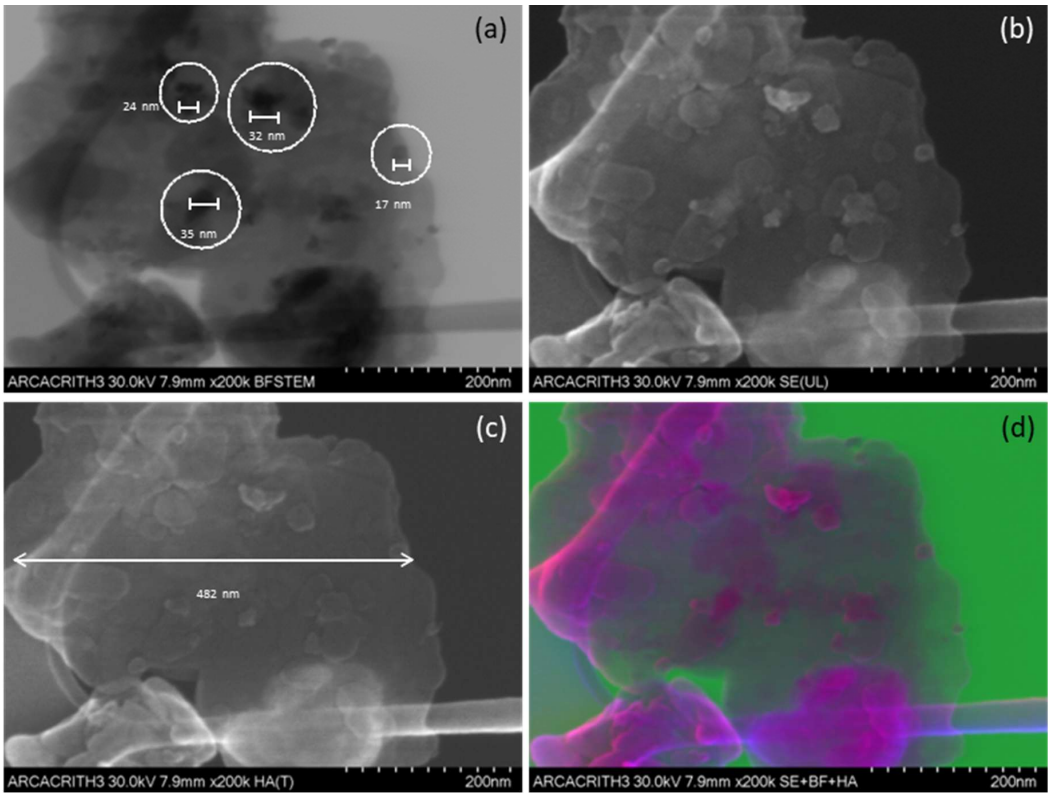

Figure 6. STEM analysis of clays of acid soil from Tabasco. (a) kaolinite phases, (b) surface topography, c) denser iron and aluminum oxides, and d) an integrated view of the sample.

In the clay fraction, kaolinite is the main aluminosilicate. Iron and aluminum oxides also adsorb strongly to the kaolinite surface, which may explain its low CEC. Aluminum and iron particles give a clay-like texture. Magnetite nanoparticles have two possible origins: annual agricultural burning in the presence of soil organic matter (Iniesta-Martínez, García, Gutiérrez, and Abud, 2023) and bacterial neoformation or pedogenetic in tropical conditions (Maher and Taylor, 1988; Preetz, Igel, Hannam, and Stadler, 2017).

Strong weathering of soil minerals with good drainage releases of Fe and Al ions, forming secondary minerals such as gibbsite and Fe oxides (goethite and hematite), and the prevalence of kaolinite (Tardy and Roquin, 1992). The CEC is low for two reasons: the type of aluminosilicate (kaolinite) and the adsorption of iron and aluminum oxides to the kaolinite, which does not fully quantify the CEC.

Fourier Transform Infrared Spectroscopy (FT-IR) Analysis

The obtained infrared spectrum exhibited characteristic absorption bands that correlate well with these mineral phases, supporting the crystalline structures determined by XRD.

In the low-wavenumber region (<1000 cm^{-1}), the absorption bands at 463 cm^{-1} and 521 cm^{-1} correspond to Si-O bending vibrations of kaolinite and Fe-O stretching vibrations of maghemite/magnetite, respectively (Figure 8). The band evidences the presence of gibbsite at 680 cm^{-1}, assigned to the Al-OH bending mode. Additionally, the absorption at 746 cm^{-1} is associated with Al-O-Si vibrations, further confirming the presence of kaolinite. The mid-range region (900-1200 cm^{-1}) exhibits prominent peaks at 911 cm^{-1}, 1001 cm^{-1}, 1032 cm^{-1}, and 1118 cm^{-1}, which are attributed to Al-OH bending vibrations in kaolinite and gibbsite, as well as Si-O stretching modes in kaolinite. These results align with the XRD findings, where characteristic diffraction peaks of kaolinite and gibbsite were observed, confirming their significant presence in the sample. The high-wavenumber region (3300-3700 cm^{-1}) reveals multiple absorption bands at 3375 cm^{-1}, 3393 cm^{-1}, and 3443 cm^{-1}, which are assigned to O-H stretching vibrations associated with adsorbed water in kaolinite and gibbsite. The peaks at 3531 cm^{-1}, 3621 cm^{-1}, 3650 cm^{-1}, and 3695 cm^{-1} correspond to structural hydroxyl groups within kaolinite and gibbsite, in agreement with their layered hydroxylated nature as confirmed by XRD.

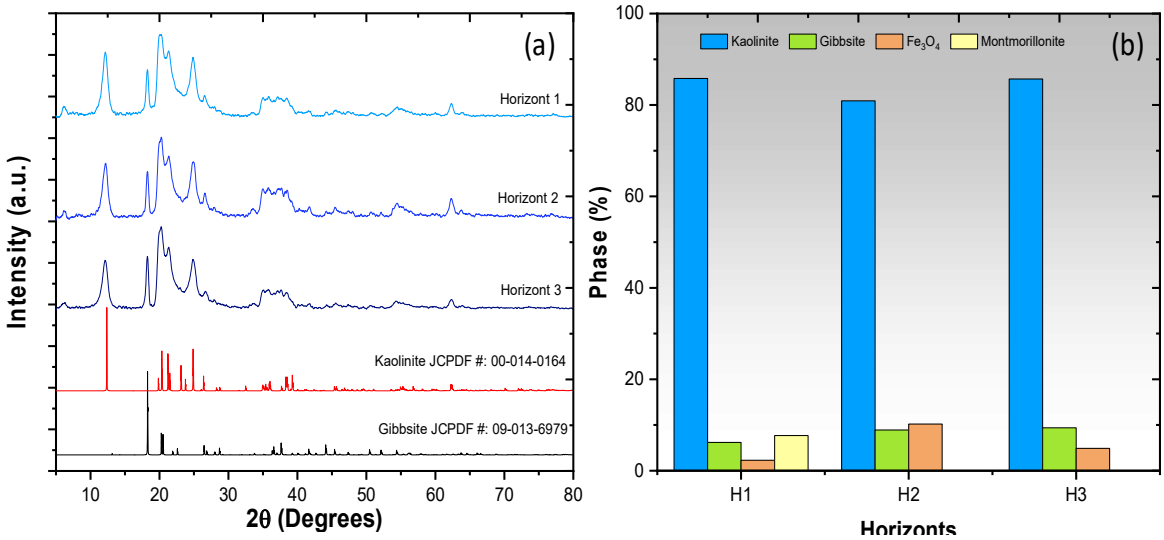

Figure 7. (a) XRD patterns of crystalline clay particles from three horizons (H1, H2, and H3) of an acid soil from Tabasco, with indexed peaks corresponding to kaolinite, gibbsite, magnetite, and montmorillonite. (b) Phase quantification showing the mineral composition of each horizon.

The correlation between FT-IR and XRD analyses highlights the mineralogical composition of particles less than 2 microns. The strong absorption features associated with kaolinite and gibbsite in FT-IR spectra validate the dominance of these minerals, as also evidenced by the XRD diffraction patterns. Additionally, the characteristic Fe-O vibrations observed in FT-IR corroborate the identification of maghemite/magnetite in XRD, confirming the presence of iron oxides in the soil matrix. These findings provide a comprehensive understanding of the mineralogical characteristics of the clay particles, demonstrating a highly weathered soil profile dominated by aluminum and iron-bearing phases, consistent with its pedogenetic development under tropical conditions.

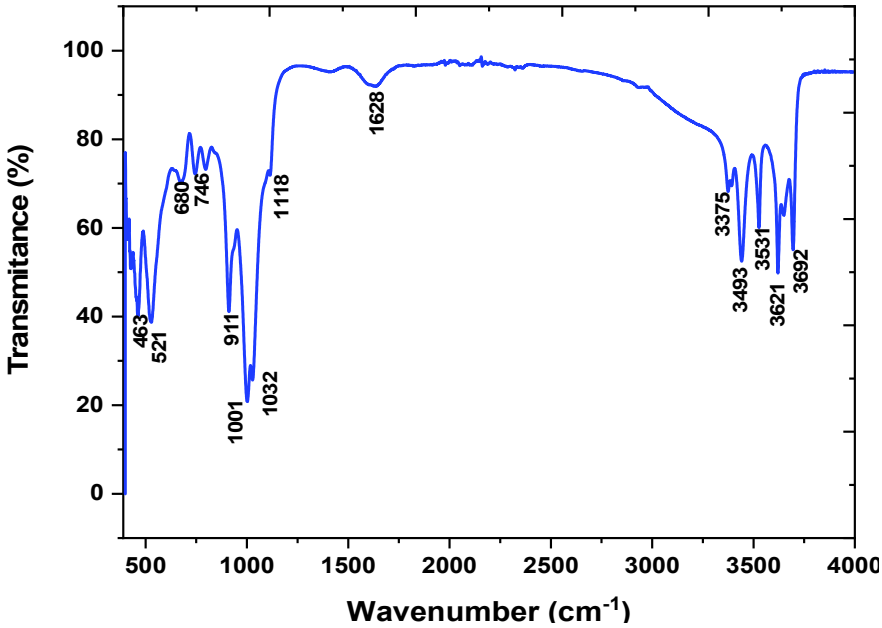

Figure 8. FT-IR spectrum of clay particles showing characteristic absorption bands of kaolinite, gibbsite, and maghemite. Key vibrations include Si-O bending (463, 521 cm^{-1}), Fe-O stretching (680, 746 cm^{-1}), Al-OH bending (911 cm^{-1}), Si-O stretching (1001, 1032, 1118 cm^{-1}), and O-H stretching (3375–3695 cm^{-1}).

Acidic Soils of Tabasco

In the state of Tabasco, Mexico, there are acidic soils that belong to the Acrisols, Luvisols, Umbrisols, and Alisols groups. Although these soils share low pH values, their morphology, functions, and agricultural uses vary significantly.

The INEGI soil database shows a well-represented cartographic distribution of Acrisols. Their properties, including the Bt horizon, cation exchange capacity (CEC), and acidity, were sufficient to classify them as such. However, with the emergence of the WRB in 1998 and its subsequent updates 2002, 2016, 2018, 2022, the mapped area of Acrisols has decreased. Some soils have even ceased to be classified as Acrisols, as the WRB (IUSS Working Group WRB, 2022) now requires a CEC (determined by 1 M NH4OAc at pH 7) of less than 24 cmol(+) kg^{-1} clay in a subhorizon of the argic horizon, along with exchangeable aluminum greater than the sum of exchangeable calcium, magnesium, potassium, and sodium. Few laboratories in the region perform these specific analyses.

The profile studied, consistent with the WRB-2022 system (IUSS Working Group WRB, 2022), is classified as a Ferric Rhodic Ferralic Acrisol (Clayic, Cutanic, Humic, Hyperdystric, Profondic). This profile features a 15 cm thick A horizon, while the argic horizon is located between 30 and 114 cm in depth. This horizon contains 24% more clay than the overlying horizon and exhibits eluviated cutans. Between 57 and 100 cm deep, the soil demonstrates an exchangeable acidity of 1.8 cmol(+) kg^{-1}, which exceeds the sum of exchangeable bases (0.8 cmol(+) kg^{-1}). The CEC is measured at 12 cmol(+) kg^{-1} clay, which is below the 24 cmol(+) kg^{-1} clay threshold. It exhibits a red color (2.5YR 4/8), an acidic pH of 4.4, a sandy clay texture, and low base saturation (less than 50%) throughout most of the profile between 50 and 100 cm deep. This profile aligns with the characteristics of Acrisols found in the ancient terraces of Huimanguillo (Zavala-Cruz *et al*., 2014; Palma-López et al., 2017).

Agricultural Management

Although it may seem contradictory, these clayey soils have very low CECs because the clay is kaolinite (Tinal-Ortiz *et al*., 2020). The CEC is the negative electric charge of clays and soil organic matter and can be permanent or pH-dependent (Cruz-Macías *et al*., 2020), which helps explain why low-activity clays such as kaolinite may result in low CEC values in acidic conditions. The high percentage of organic matter is due to the formation of recalcitrant organo-mineral compounds with sand, silt, and clay particles. However, this organic matter neither provides nutrients nor promotes an increase in CEC.

In this study, we observed a large amount of iron and aluminum oxide nanoparticles on the surface of clay and silt particles. The low cation exchange capacity in this soil may be due to the lack of desorption of iron nanoparticles, so it will be necessary to study this phenomenon in future studies. Also, iron and aluminum oxides can be occluded/adsorbed by phosphate (Claudio, Iorio, Liu, and Violante, 2017), more iron than aluminum oxide (Gypser, Hirsch, Schleicher, and Freese, 2018).

The primary minerals in fine earth are found in sand and silt, since clays are considered secondary minerals that can absorb nutrients but do not contain them in their mineral structure. Between sand and silt, the silts are the most weatherable because they have a larger surface area (Hardy and Cornu, 2006; Makabe, *et al*., 2009). The weathering of the primary minerals contained in silt is the soil's nutrient reserve (Wilson, 2004; Makabe *et al*., 2009). In our case study, the elemental content in silt presented the following sequence: O > Al > Si > C > Fe > Ag > Na > Ti > Mg > Ca, where nutrients are clearly at the end of the sequence.

Given the soil conditions such as its acidity, low CEC, low percentage of silts with primary minerals with low nutrient content, as well as the high annual rainfall of 2600 mm (López-Castañeda, Zavala, Palma, Rincón, and Bautista, 2022), the following is recommended: a) select crops adapted to the environment, such as citrus, pineapple, cassava and pastures, as well as eucalyptus and rubber forest plantations (López-Reyes *et al*., 2016; Salgado-García *et al*., 2017; Tinal-Ortiz *et al*., 2020); b) fractionally apply fertilization according to crop development; and c) If the choice is to increase soil pH, the use of agricultural dolomite is recommended for its calcium and magnesium content, and the use of wastewater with a high organic and nutrient load, such as the vinasse generated in sugar/alcohol mills (Bautista-Zúñiga and Del Carmen Duran, 1998; Bautista-Zúniga, Del Carmen Durán, and Lozano, 2000). Mineral fertilization is essential due to the low levels of exchangeable cations and the limited content of primary minerals such as Ca^{2+}, Mg^{2+}, and K^{+} in the silt and sand fractions.

Acrisols are classified as III or IV in plains but are V and VI in hills (Palma-López, Cisneros, Moreno, and Rincón, 2007); however, with good crop selection and better management of soil fertility, it will be possible to improve one or two classes of agricultural use capacity.

On the other hand, we find organic matter bound to sand, silt, and clay particles, forming organomineral compounds, which is why organic matter retention is high. It has been reported that organic matter is retained primarily in particles smaller than 20 microns (silt and clay) (Zhao, Sun, Zhang, and Yang, 2006; Claudio *et al*., 2017; Matus, 2021). However, in this study, even sand particles can retain organic matter, perhaps due to iron and aluminum minerals.

CONCLUSIONS

For the first time, the shape, size, and mineral and elemental composition of sand and silt particles in acidic soils in Tabasco, Mexico, have been characterized. Although the techniques used in this study have been widely reported for other soils around the world. Clay particles, such as kaolinite and iron and aluminum oxides, had already been identified indirectly by low CEC and by chemical extractions, respectively; however, the presence of these particles has now been confirmed by XRD. The presence of magnetite is reported for the first time.

The acidic soils of Tabasco are of great importance to local agriculture, unfortunately, their function was not well understood. On the one hand, they are clayey soils, but on the other, they have low cation exchange capacity (CEC) values, in addition to a low percentage of silt, and therefore low weatherable mineral reserves in the medium term.

The results of this work show that the sand particles presented irregular shapes, with silicon (Si) and oxygen (O), probably quartz and aluminum (Al), as well as iron (Fe) and carbon present in low proportions. Due to the high percentage of sand in the soil, there is no drainage problem.

Silt particles between 2 and 63 microns showed a sequence of elements of the type O> Al> Si> C> Fe> Ag> Na> Ti> Mg> Ca, and organo-mineral compounds associated with primary and secondary minerals were also found. The low percentage of silt to make thinking that the nutrient reserve in soil is low, which is consistent with the widespread practice of adding lime.

The particles smaller than 2 microns are aluminosilicate as kaolinite, plus nanometric particles of gibbsite, magnetite, and iron sesquioxide's. Nanoparticles are found on the surface of the kaolinite. We find smectite but only in the surface horizon and in low proportions.

ETHICS STATEMENT

Not applicable.

CONSENT FOR PUBLICATION

Not applicable.

AVAILABILITY OF SUPPORTING DATA

The datasets used and analyzed during the current study are available from the corresponding author on reasonable request.

COMPETING INTERESTS

The authors declare that they have no competing interests.

FINANCING

DGAPA Universidad Nacional Autónoma de México, Grant No. IN208621 and SECIHTI project CBF2023-2024-410 funded this research.

AUTHORS' CONTRIBUTIONS

Formal analysis, Data curation, Resources, Investigation, Visualization, and Writing – review and editing: A.L.C.; Formal analysis, Software, Methodology, Resources, Investigation, and Writing – review and editing: A.J.R.B.; Investigation (sampling), Resources, Visualization, Supervision, and Writing – review and editing: D.J.P.L.; Resources, Investigation (sampling), Supervision, Visualization, and Writing – review and editing: J.Z.C.; Conceptualization, Investigation, Supervision, Project administration, Funding acquisition, and Writing – review and editing: F.B.Z.

ACKNOWLEDGMENTS

Alvaro de Jesús agradece el apoyo a la SECIHTI en colaboración con CFATA, por el apoyo brindado mediante el programa investigadoras e investigadores por México SECIHTI

REFERENCES

Aceves-Navarro, L. A., & Rivera-Hernández, B. (2019). Clima. En E. E. Mata-Zayas & D. J. Palma-López (Eds.). *La biodiversidad en Tabasco. Estudio de estado* (pp. 61-68). Villahermosa, Tabasco, México: Comisión Nacional para el Conocimiento y Uso de la Biodiversidad (CONABIO) y Gobierno del Estado de Tabasco.

Adhikari, G., & Bhattacharyya, K. G. (2015). Correlation of soil organic carbon and nutrients (NPK) to soil mineralogy, texture, aggregation, and land use pattern. *Environmental Monitoring and Assessment, 187*(11), 735. https://doi.org/10.1007/s10661-015-4932-5

Agegnehu, G., Amede, T., Erkossa, T., Yirga, C., Henry, C., Tyler, R., ... & Sileshi, G. W. (2021). Extent and management of acid soils for sustainable crop production system in the tropical agroecosystems: a review. *Acta Agriculturae Scandinavica, Section B—Soil & Plant Science, 71*(9), 852-869.

Bautista-Zúñiga, F., & Del Carmen Durán-De Bazúa, M. (1998). Análisis del beneficio y riesgo potenciales de la aplicación al suelo de vinazas crudas y tratadas biológicamente. *Revista Internacional de Contaminación Ambiental, 14*(1), 13-19.

Bautista-Zúniga, F., Del Carmen Durán-De Bazúa, M., & Lozano, R. (2000). Cambios químicos en el suelo por aplicación de materia orgánica soluble tipo vinazas. *Revista Internacional de Contaminación Ambiental, 16*(3), 89-101.

Bremner, J. M., & Genrich, D. A. (1990). Characterisation of the sand, silt, and clay fractions of some Mollisols. In M. E. Sumner & C. B. Stewart (Eds.). *Soil colloids and their associations in aggregates* (pp. 423-438). New York, NY, USA: Springer US.

Castillo, S., Popma, J., & Moreno-Casasola, P. (1991). Coastal sand dune vegetation of Tabasco and Campeche, Mexico. *Journal of Vegetation Science, 2*(1), 73-88.

Claudio, C., Iorio, E. D., Liu, Q., Jiang, Z., & Barron, V. (2017). Iron oxide nanoparticles in soils: Environmental and agronomic importance. *Journal of Nanoscience and Nanotechnology, 17*(7), 4449-4460.

Cruz-Macías, W. O., Rodríguez-Larramendi, L. A., Salas-Marina, M. Á., Hernández-García, V., Campos-Saldaña, R. A., Chávez-Hernández, M. H., & Gordillo-Curiel, A. (2020). Efecto de la materia orgánica y la capacidad de intercambio catiónico en la acidez de suelos cultivados con maíz en dos regiones de Chiapas, México. *Terra Latinoamericana, 38*(3), 475-480. https://doi.org/10.28940/terra.v38i3.506

Delmelle, P., Opfergelt, S., Cornelis, J. T., & Ping, C. L. (2015). Volcanic soils. In H. Sigurdsson (Ed.). *The encyclopedia of volcanoes* (pp. 1253-1264). Amsterdam, The Netherlands: Academic Press.

Djeran-Maigre, I., Razakamanantsoa, A., Levacher, D., Hussain, M., & Delfosse, E. (2023). A relevant characterization of Usumacinta river sediments for a reuse in earthen construction and agriculture. *Journal of South American Earth Sciences, 125*, 104317. https://doi.org/10.1016/j.jsames.2023.104317

Feng, M., Kou, Z., Tang, C., Shi, Z., Tong, Y., & Zhang, K. (2023). Recent progress in synthesis of zeolite from natural clay. *Applied Clay Science, 243*, 107087. https://doi.org/10.1016/j.clay.2023.107087

Geissen, V., Sánchez-Hernández, R., Kampichler, C., Ramos-Reyes, R., Sepulveda-Lozada, A., Ochoa-Goana, S., ... & Hernández-Daumas, S. (2009). Effects of land-use change on some properties of tropical soils-an example from Southeast Mexico. *Geoderma, 151*(3-4), 87-97. https://doi.org/10.1016/j.geoderma.2009.03.011

Graham, E. R. (1943). Soil development and plant nutrition: II. Mineralogical and chemical composition of sand and silt separates in relation to the growth and chemical composition of soybeans. *Soil Science, 55*(3), 265.

Gypser, S., Hirsch, F., Schleicher, A. M., & Freese, D. (2018). Impact of crystalline and amorphous iron- and aluminum hydroxides on mechanisms of phosphate adsorption and desorption. *Journal of Environmental Sciences, 70*, 175-189.

Hardy, M., & Cornu, S. (2006). Location of natural trace elements in silty soils using particle-size fractionation. *Geoderma, 133*(3-4), 295-308.

Hassink, J. (1997). The capacity of soils to preserve organic C and N by their association with clay and silt particles. *Plant and Soil, 191*(1), 77-87.

Iniesta-Martínez, L., García-Ruiz, R., Sánchez, R., Goguitchaichvili, A., & Bautista, F. (2023). El magnetismo y el color como indicadores de cambios en el suelo por quema agrícola. *Boletín de la Sociedad Geológica Mexicana, 75*(2), A050523.

Islas-Tenorio, J. J., Ramírez-García, M. G., Gómez-Ávilez, A., Moreno-Ruíz, J. P., Wingartz-Carranza, J. A., & Mendieta-Flores, J. L. (2005). *Carta geológico-minera Villahermosa E15-8 escala 1:250 000*. Pachuca, Hidalgo, México: Servicio Geológico Mexicano.

IUSS Working Group WRB. (2022). *World Reference Base for Soil Resources: International soil classification system for naming soils and creating legends for soil maps* (4th ed.). Vienna, Austria: International Union of Soil Sciences (IUSS).

Liu, J., Wang, Z., Hu, F., Xu, C., Ma, R., & Zhao, S. (2020). Soil organic matter and silt contents determine soil particle surface electrochemical properties across a long-term natural restoration grassland. *Catena, 190*, 104526. https://doi.org/10.1016/j.catena.2020.104526

López-Castañeda, A., Zavala-Cruz, J., Palma-López, D. J., Rincón-Ramírez, J. A., & Bautista, F. (2022). Digital mapping of soil profile properties for precision agriculture in developing countries. *Agronomy, 12*(2), 353. https://doi.org/10.3390/agronomy12020353

López-Reyes, L. Y., Domínguez-Domínguez, M., Martínez-Zurimendi, P., Zavala-Cruz, J., Gómez-Guerrero, A., & Posada-Cruz, S. (2016). Carbono almacenado en la biomasa aérea de plantaciones de hule (*Hevea brasiliensis Müell*. Arg.) de diferentes edades. *Madera y Bosques, 22*(3), 49–60.

Maher, B. A., & Taylor, R. M. (1988). Formation of ultrafine-grained magnetite in soils. *Nature, 336*(6197), 368–370.

Marín-Mézquita, L., Baeza, L., Zapata-Pérez, O., & Gold-Bouchot, G. (1997). Trace metals in the American oyster, Crassostrea virginica, and sediments from the coastal lagoons Mecoacan, Carmen and Machona, Tabasco, Mexico. *Chemosphere, 34*(11), 2437-2450. https://doi.org/10.1016/S0045-6535(97)00046-5

Makabe, S., Kakuda, K. I., Sasaki, Y., Ando, T., Fujii, H., & Ando, H. (2009). Relationship between mineral composition or soil texture and available silicon in alluvial paddy soils on the Shounai Plain, Japan. *Soil Science and Plant Nutrition, 55*(2), 300-308. https://doi.org/10.1111/j.1747-0765.2008.00352.x

Matus, F. J. (2021). Fine silt and clay content is the main factor defining maximal C and N accumulations in soils: a meta-analysis. *Scientific Reports, 11*(1), 6438. https://doi.org/10.1038/s41598-021-84821-6

Mendoza-Carranza, M., Sepúlveda-Lozada, A., Dias-Ferreira, C., & Geissen, V. (2016). Distribution and bioconcentration of heavy metals in a tropical aquatic food web: A case study of a tropical estuarine lagoon in SE Mexico. *Environmental Pollution, 210*, 155-165. https://doi.org/10.1016/j.envpol.2015.12.014

Miaomiao, X. U., Xiaochun, W. E. I., Rong, Y. A. N. G., Ping, W. A. N. G., & Xiaogan, C. H. E. N. G. (2021). Research progress of provenance tracing method for heavy mineral analysis. *Advances in Earth Science, 36*(2), 154-171. https://doi.org/10.11867/j.issn.1001-8166.2021.021

Mora, J. L., Guerra, J. A., Armas-Herrera, C. M., Arbelo, C. D., & Rodríguez-Rodríguez, A. (2014). Storage and depth distribution of organic carbon in volcanic soils as affected by environmental and pedological factors. *Catena, 123*, 163-175. https://doi.org/10.1016/j.catena.2014.08.004

Nie, Q., Li, Y., Wang, G., & Bai, B. (2020). Physicochemical and microstructural properties of red muds under acidic and alkaline conditions. *Applied Sciences, 10*(9), 2993. https://doi.org/10.3390/app10092993

Palma-López, D. J., Cisneros, D. J., Moreno, C. E., & Rincón-Ramírez, J. A. (2007). *Suelos de Tabasco: Su uso y manejo sustentable*. Montecillo, Texcoco, Estado de México, México: Colegio de Postgraduados-ISPROTAB-FUPROTAB.

Palma-López, D. J., Moreno C., E., Rincón-Ramírez, J. A., & Shirma-Torres, E. D. (2008). *Degradación y conservación de los suelos del estado de Tabasco*. Villahermosa, Tabasco, México: Colegio de Postgraduados-Campus Tabasco, CONACYT, CCYTET. ISBN: 978-968-839-611-7.

Palma-López, D. J., Jiménez-Ramírez, R., Zavala-Cruz, J., Bautista-Zuñiga, F., Gavi-Reyes, F., & Palma-Cancino, D. Y. (2017). Actualización de la clasificación de suelos de Tabasco, México. *Agroproductividad, 10*(12), 29-35.

Prado, B., Duwig, C., Hidalgo, C., Gómez, D., Yee, H., Prat, C., … & Etchevers, J. D. (2007). Characterization, functioning and classification of two volcanic soil profiles under different land uses in Central Mexico. *Geoderma, 139*(3-4), 300-313. https://doi.org/10.1016/J.GEODERMA.2007.02.008

Preetz, H., Igel, J., Hannam, J. A., & Stadler, S. (2017). Relationship between magnetic properties and reddening of tropical soils as indicators of weathering. *Geoderma, 303*, 143-149. https://doi.org/10.1016/j.geoderma.2017.05.007

Ramos-Vázquez, M. A., & Armstrong-Altrin, J. S. (2020). Provenance and palaeoenvironmental significance of microtextures in quartz and zircon grains from the Paseo del Mar and Bosque beaches, Gulf of Mexico. *Journal of Earth System Science, 129*(1), 225.

Salgado-García, S., Palma-López, D. J., Zavala-Cruz, J., Ortiz-García, C. F., Lagunes-Espinoza, L. C., Ortiz-Ceballos, A. I., ... & Salgado-Velázquez, S. (2017). Los suelos ácidos de la sabana de Huimanguillo, Tabasco, México. *Agro Productividad, 10*(12), 16-21.

Sánchez, P. A., & Logan, T. J. (1992). Myths and science about the chemistry and fertility of soils in the Tropics. En R. Lal & P. A. Sanchez (Eds.). *Myths and science of soils of the Tropics* (pp. 35–46). Madison, WI, USA: Soil Science Society of America.

Soares, M. R., Alleoni, L. R., Vidal-Torrado, P., & Cooper, M. (2005). Mineralogy and ion exchange properties of the particle size fractions of some Brazilian soils in tropical humid areas. *Geoderma, 125*(3-4), 355-367. https://doi.org/10.1016/j.geoderma.2004.09.008

Tardy, Y., & Roquin, C. (1992). Geochemistry and evolution of lateritic landscapes. In I. P. Martini & W. Chesworth (Eds.). *Weathering, soils & paleosols* (pp. 407-443). Amsterdam, The Netherlands: Elsevier.

Thaymuang, W., Kheoruenromne, I., Suddhipraharn, A., & Sparks, D. L. (2013). The role of mineralogy in organic matter stabilization in tropical soils. *Soil Science, 178*(6), 308–315.

Tinal-Ortiz, S., López, D. J. P., Zavala-Cruz, J., Salgado-García, S., Palma-Cancino, D. J., & Hidalgo-Moreno, C. I. (2020). Degradación química en Acrisoles bajo diferentes usos y pendientes en la sabana de Huimanguillo, Tabasco, México. *Agro Productividad, 13*(2), 1-7.

von Uexküll, H. R., & Mutert, E. (1995). Global extent, development and economic impact of acid soils. *Plant and Soil, 171*(1), 1–15. https://doi.org/10.1007/BF00009558

Villanueva-Partida, C., Casanova-Lugo, F., Villanueva-López, G., González-Valdivia, N., Oros-Ortega, I., & Díaz-Echeverría, V. (2016). Influence of the density of scattered trees in pastures on the structure and species composition of tree and grass cover in southern Tabasco, Mexico. *Agriculture, Ecosystems & Environment, 232*, 1-8. https://doi.org/10.1016/j.agee.2016.07.020

Villasenor, R., Magdaleno, M., Quintanar, A., Gallardo, J. C., López, M. T., Jurado, R., ... & Barchet, W. R. (2003). An air quality emission inventory of offshore operations for the exploration and production of petroleum by the Mexican oil industry. *Atmospheric Environment, 37*(26), 3713-3729.

Wilson, M. J. (2004). Weathering of the primary rock-forming minerals: processes, products and rates. *Clay Minerals, 39*(3), 233-266.

Zavala-Cruz, J., Jiménez Ramírez, R., Palma-López, D. J., Bautista Zúñiga, F., & Gavi Reyes, F. (2016). Paisajes geomorfológicos: base para el levantamiento de suelos en Tabasco, México. *Ecosistemas y Recursos Agropecuarios, 3*(8), 161-171.

Zavala-Cruz, J., Salgado-García, S., Marín-Aguilar, Á., Palma-López, D. J., Castelán-Estrada, M., & Ramos-Reyes, R. (2014). Transecto de suelos en terrazas con plantaciones de cítricos en Tabasco. *Ecosistemas y Recursos Agropecuarios, 1*(2), 123-137.

Zhao, L., Sun, Y., Zhang, X., Yang, X., & Drury, C. F. (2006). Soil organic carbon in clay and silt sized particles in Chinese mollisols: Relationship to the predicted capacity. *Geoderma, 132*(3-4), 315-323. https://doi.org/10.1016/j.geoderma.2005.04.026

Zhu, Y., Guo, B., Liu, C., Lin, Y., Fu, Q., Li, N., & Li, H. (2021). Soil fertility, enzyme activity, and microbial community structure diversity among different soil textures under different land use types in coastal saline soil. *Journal of Soils and Sediments, 21*(6), 2240-2252. https://doi.org/10.1007/s11368-021-02916-z